JOURNAL OF MAGNETIC RESONANCE **129,** 30–34 (1997)
ARTICLE NO. MN971254

Coherence Sidebands in Adiabatic Decoupling

M. Robin Bendall and Thomas E. Skinner*

*Department of Chemistry and Chemical Engineering, School of Molecular Sciences, James Cook University of North Queensland, Townsville, 4811 Queensland, Australia; and *Physics Department, Wright State University, Dayton, Ohio 45435*

Received April 28, 1997

RF pulse sequences applied to IS spin systems may produce substantial transverse antiphase S magnetization coupled to antiphase I magnetization, just prior to detection of the S signal, for samples containing a range of J coupling constants, or when pulse sequence delays are misset from ideal values. This magnetization is generally considered to be unobservable. Adiabatic decoupling on the I spins during signal detection efficiently converts this magnetization to observable S signal in the form of sidebands which we dub "coherence sidebands." Three single-transient pulsed-field-gradient methods are described for eliminating these unwanted sidebands. The techniques are applicable to ^{1}H-detected ^{13}C-decoupled experiments on spectrometers operating at a ^{1}H frequency of up to 2 GHz. © 1997 Academic Press

Recently (*1*), we reported an effect, also seen in composite-pulse decoupling (*2*), that significantly degrades the performance of all adiabatic decoupling schemes. If the pulse sequence prior to decoupling creates order in the S spins relative to the I spins, subsequent coherent decoupling of the I spins may convert this order to additional sideband intensity. Since these sidebands are induced by the IS pulse sequence prior to decoupling, we will refer to them as ''coherence sidebands.'' The problem is not readily apparent in evaluations of decoupling performance applied to idealized samples containing a single value of the coupling constant J. The preparation pulse sequence in these cases is typically optimized for the particular value of J, producing only in-phase magnetization at the start of signal acquisition. In real samples with a range of coupling constants, antiphase magnetization is also produced by the preparation sequence, and we find that maximum sideband intensity at each resonance offset over the entire decoupled bandwidth can increase by almost an order of magnitude compared to the ideal value attainable at a single value of J. The effect thus presents a serious threat to the utility of adiabatic decoupling sequences. Asynchronous decoupling, as used in composite pulse methods, is not a viable solution to the problem, since it actually degrades the performance of adiabatic decoupling (*3*). A phase-cycling method using hard inversion pulses was proposed (*2*) to reduce the effects of coherence sidebands in composite-pulse decoupling. The bilevel adiabatic decoupling scheme (*4*), recently introduced as a method for canceling ordinary sidebands resulting from in-phase magnetization, is also a signal-averaging technique that has been demonstrated to be effective on or near resonance and might be more generally applicable. For now, we will emphasize methods that eliminate coherence sidebands in a single transient over bandwidths appropriate to modern broadband decoupling.

The importance of eliminating antiphase responses in certain circumstances is well known. Pegg *et al.* (*5*) described the use of short bursts of noise decoupling to randomize spins and cancel antiphase magnetization across the sample via the spatial inhomogeneity of the RF field. They provided details of experimental conditions for complete randomization using RF probes that are much less homogeneous than the present-day standard. A detailed description of the conditions under which longitudinal antiphase magnetization at the end of a decoupled evolution period could affect the amplitude and/or phase of the detected signal was provided by Levitt *et al.* (*6*). These particular effects were noted to be undetectable in 1D spectra if the decoupler was applied continuously during acquisition, in direct contrast to our observations of coherence sidebands using adiabatic decoupling.

The subject of this article is a related phenomenon that is apparent whenever either longitudinal or transverse antiphase magnetization is present at the start of a decoupled acquisition. If the S spins in an IS system are prepared pure antiphase, both multiplet components having the same amplitude, adiabatic decoupling produces no signal at the frequency of the centerband, as expected. However, we show that the decoupler irradiation applied to the I spins transforms unobservable quantum coherence into observable and reproducible S-spin signal in the form of sidebands. The magnitude of the problem is first demonstrated using a heteronuclear spin-echo difference experiment (*7*). The existence of coherence sidebands is then accounted for by a standard density matrix calculation of the detected signal, given the appropriate initial conditions at the start of the decoupling period. Finally, methods for eliminating these sidebands in a single transient are verified experimentally over the full

1090-7807/97 $25.00

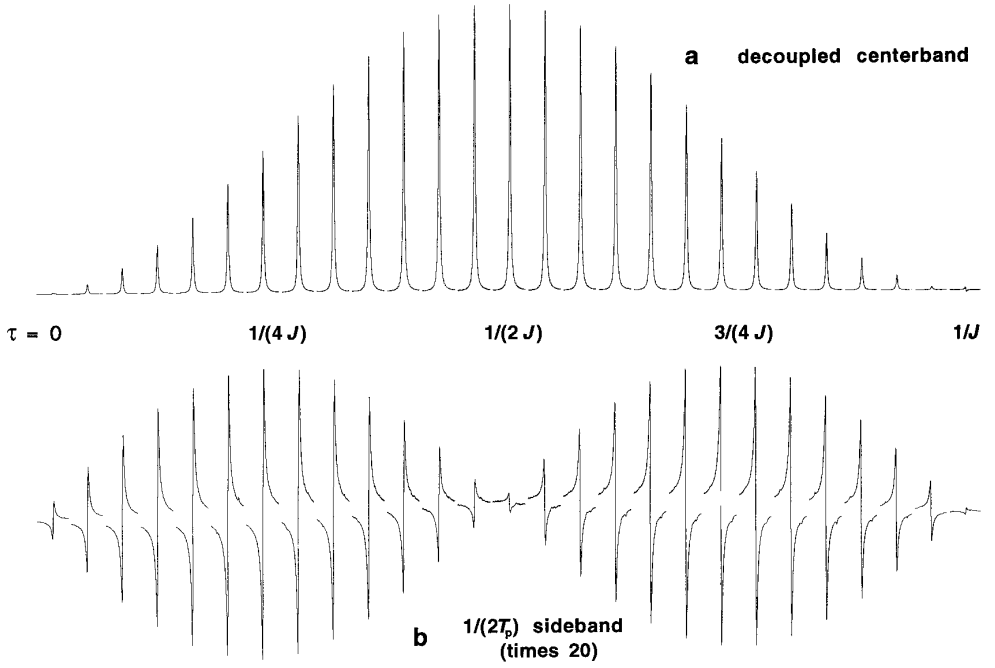

FIG. 1. Spectra obtained at incremented τ times using the heteronuclear spin-echo difference pulse sequence (*7*) followed by STUD decoupling (RF_{max} = 10 kHz, the maximum B_1 amplitude; T_p = 1.1 ms, the length of a single adiabatic inversion pulse; bwdth = 50 kHz, the total frequency sweep during the pulse). The results were obtained from ^{1}H-detected ^{13}C-decoupled spectra (two transients) generated using a sample of $^{13}CH_3I$ (J_{CH} = 150 Hz) in a 5-mm HCN triple-resonance PFG probe on a 500-MHz Varian INOVA spectrometer. (a) The decoupled centerband. (b) The sideband at $1/(2T_p)$ downfield from the centerband, with the vertical scale multiplied by 20 relative to (a).

decoupled bandwidth applicable to a spectrometer operating at up to 2 Ghz.

Consider an experiment that observes the *x* component of S-spin magnetization while decoupling I spins. An example is provided in Fig. 1 for on-resonance decoupling of $^{13}CH_3I$ (J_{CH} = 150 Hz) following a heteronuclear spin-echo difference sequence. In what follows, even-numbered transients refocus both chemical shift and *J* coupling, while odd transients refocus chemical shift only. Details of the experiment and decoupling parameters can be found in the figure legend. As usual, we discuss adiabatic decoupling in terms of RF_{max}, the maximum B_1 amplitude in hertz; bwdth, the total frequency range swept during an adiabatic inversion pulse; and T_p, the length of the pulse in seconds. At the top of the figure, the experimental decoupled peak is plotted as a function of the τ delay, showing the usual *J* modulation of the signal. For the optimal setting $\tau = 1/(2J)$, the maximum sideband intensity is found to be $\approx$0.6% at an offset of $1/T_p$, where both amplitude and offset are measured relative to the central decoupled peak. Figure 1b shows the additional sideband intensity that is induced at $1/(2T_p)$ as a function of the τ delay. This sideband has a maximum value of 4.6% at $\tau = 1/(4J)$, and $3/(4J)$, and is larger than the $1/T_p$ sideband at all delays except $\tau = 1/(2J)$, where its amplitude is close to zero. Broadband adiabatic decoupling will be most commonly used for ^{13}C decoupling during ^{1}H detection. Coupling constants vary from 125 to 220 Hz, so using a compromise value of J = 150 Hz to set the $1/(2J)$ period gives a corresponding variation of $0.4/J$ to $0.7/J$ in the optimal delay times for the various constituents in the sample. Thus, according to Fig. 1, coherence sidebands will commonly arise at levels close to maximum.

In the absence of quantum-coherence terms, such as when the τ delay is set correctly in the spin-echo difference experiment, the initial density matrix, ρ_0, is represented by the in-phase term, S_x. The detected signal is proportional to the expectation value of S_x, and for S spins on resonance one obtains (*8*)

$$\langle S_x(t)\rangle \propto (1 + \mathbf{n}^+ \cdot \mathbf{n}^-)\cos\frac{\varphi^+ - \varphi^-}{2} + (1 - \mathbf{n}^+ \cdot \mathbf{n}^-)\cos\frac{\varphi^+ + \varphi^-}{2}, \qquad [1]$$

where the irradiated I spins, initially in a $\pm z$ state, are represented at each time t by a net rotation of $\varphi^{\pm}$ about an axis defined by the unit vectors $\mathbf{n}^{\pm}$. Ideal decoupling occurs for $\varphi^+ = \varphi^-$ and $\mathbf{n}^+ = \mathbf{n}^-$, in which case $\langle S_x(t)\rangle$ is constant as a function of time, representing a pure decoupled peak at zero frequency. The small deviations from the ideal case that occur for even the best decoupling sequence impose

both amplitude and frequency modulations on the signal through the time dependence of $\mathbf{n}^+ \cdot \mathbf{n}^-$ and $\varphi^+ \pm \varphi^-$, respectively. Fourier transformation reveals the frequency components of this modulation as sidebands.

If there are either longitudinal or transverse antiphase terms present at the beginning of signal acquisition, such as when τ is misset in Fig. 1 or after an HMQC sequence, then for $\rho_0 \rightarrow 2S_yI_j$ $(j = x, y, z)$, we obtain

$$\langle S_x(t)\rangle \propto (\mathbf{n}^+ + \mathbf{n}^-)_j \sin\frac{\varphi^+ - \varphi^-}{2} + (\mathbf{n}^+ - \mathbf{n}^-)_j \sin\frac{\varphi^+ + \varphi^-}{2} - (\mathbf{n}^+ \times \mathbf{n}^-)_j \times \left[\cos\frac{\varphi^+ - \varphi^-}{2} - \cos\frac{\varphi^+ + \varphi^-}{2}\right]. \quad [2]$$

Only for ideal decoupling is this result equal to zero. Otherwise, Eq. [2] indicates the existence of coherence sidebands which are different from the ordinary sidebands implied by Eq. [1]. However, $\varphi^\pm$ and $\mathbf{n}^\pm$ must be solved numerically for a given decoupling sequence and specific resonance offset of the I spins to determine the relative intensities of the sidebands. Simulations of STUD decoupling based on Eqs. [1] and [2] confirm and extend the results of Fig. 1—coherence sidebands at all decoupler offsets are significantly greater than sidebands produced starting with in-phase magnetization. In addition, sidebands resulting from longitudinal quantum coherence in the simulations were found to be greater than those produced by transverse coherence.

These conclusions are confirmed experimentally in Fig. 2, where sideband intensity is investigated over a decoupled bandwidth of almost 100 kHz. In each panel of Fig. 2, the decoupler was offset in increments of 2 kHz. Sidebands in the interval 80–1170 Hz downfield from the central decoupled peak are displayed at each offset. This window is sufficiently wide to show all the major sidebands, which are in the range $1/(10T_p)$ to $1/T_p$. At each offset, the sideband peak furthest to the left in the displayed portion of the decoupled spectrum is the $1/T_p$ sideband. The $1/(2T_p)$ sideband is just to the right of center of each segment of the displayed spectra. A complex series of sidebands begin just to the left of the $1/(2T_p)$ sideband (the middle of each window) and extend all the way to the centerband. Since these sidebands resemble noise, but are nevertheless exactly reproducible at any decoupler offset, we refer to this as ''sideband noise.'' In these examples, the dominant sideband in this noise region is the $1/(5T_p)$ sideband. Figure 2a shows the standard sidebands produced by decoupling with the optimal delay, $\tau = 1/(2J)$. The relatively flat profile of maximum sideband intensity as a function of decoupler offset is characteristic of hyperbolic secant decoupling (*1, 3*) in the absence of coherence sidebands. The maximum sideband intensity over the decoupled bandwidth is 0.7%, and the intensity of the $1/(2T_p)$ sidebands in this case is less than or equal to this value.

Figure 2b shows the large coherence sidebands that result from the presence of longitudinal coherence S_yI_z when the delay is maximally misset at $\tau = 3/(4J)$ (i.e., as in Fig. 1b), where there is no in-phase magnetization for odd transients. The $1/(2T_p)$ sideband dominates as in Fig. 1b, and the sideband noise has also increased compared to Fig. 2a. Sidebands produced by transverse coherence can be obtained for comparison by applying a hard 90° pulse to the ^{13}C spins (i.e., 90[I]) immediately before decoupling, as shown in Fig. 2c. Although the $1/(2T_p)$ sideband is substantially reduced or even eliminated in this case, the sideband noise is increased compared to Fig. 2b, so these complex coherence sidebands are still much larger than the standard sidebands of Fig. 2a.

Equation [2], and Figs. 2b and 2c, shows that the observed decoupled signal will include significant contributions from antiphase coherence. Since separate $\pm S_yI_j$ terms will cancel, this suggests a simple strategy to eliminate coherence sidebands in a single transient—either the I or the S magnetization in any initial S_yI_j term should be distributed uniformly over the interval 0 to 2π (i.e., randomized) in an appropriate plane. The technique will be effective to the extent that randomization can be produced over the full chemical shift range of either the I or the S spins. Most pulse sequences conclude with a τ delay prior to detection of the S spins, so the appropriate spins can be randomized using pulsed field gradients immediately before signal acquisition.

We first apply this method to the I spins. At the end of the spin-echo period in each odd transient, a field gradient pulse, G, was followed by a hard 90° pulse on the I spins, followed by an inverted field gradient pulse, $-G$. Longitudinal I magnetization is rotated into the transverse plane by the 90[I] pulse, and then spatially randomized by the $-G$ pulse. Transverse S-spin magnetization is unaffected because the effects of G and $-G$ cancel. The entire G; 90[I]; $-G$ sequence can be delivered in 100 μs or less, which is short with respect to the τ delay in relevant cases. Figure 2d shows the general effectiveness of this method for eliminating transverse coherence. The transmitter offset for the 90[I] pulse is equal to the decoupler offset for each interval. Sideband levels over 40 kHz of the decoupled bandwidth are approximately equal to the standard sideband levels in Fig. 2a, indicating nearly complete suppression of the coherence sidebands. The reduction in effectiveness of this technique near the edge of the decoupled bandwidth is directly related to limitations in the excitation bandwidth of a hard 90[I] pulse at frequency offsets greater than the magnitude of the RF field. For ^{13}C decoupling, a coverage of about 40 kHz is almost the maximum bandwidth required for a future 1-GHz spectrometer.

Pulsed field gradients are not available on standard probe

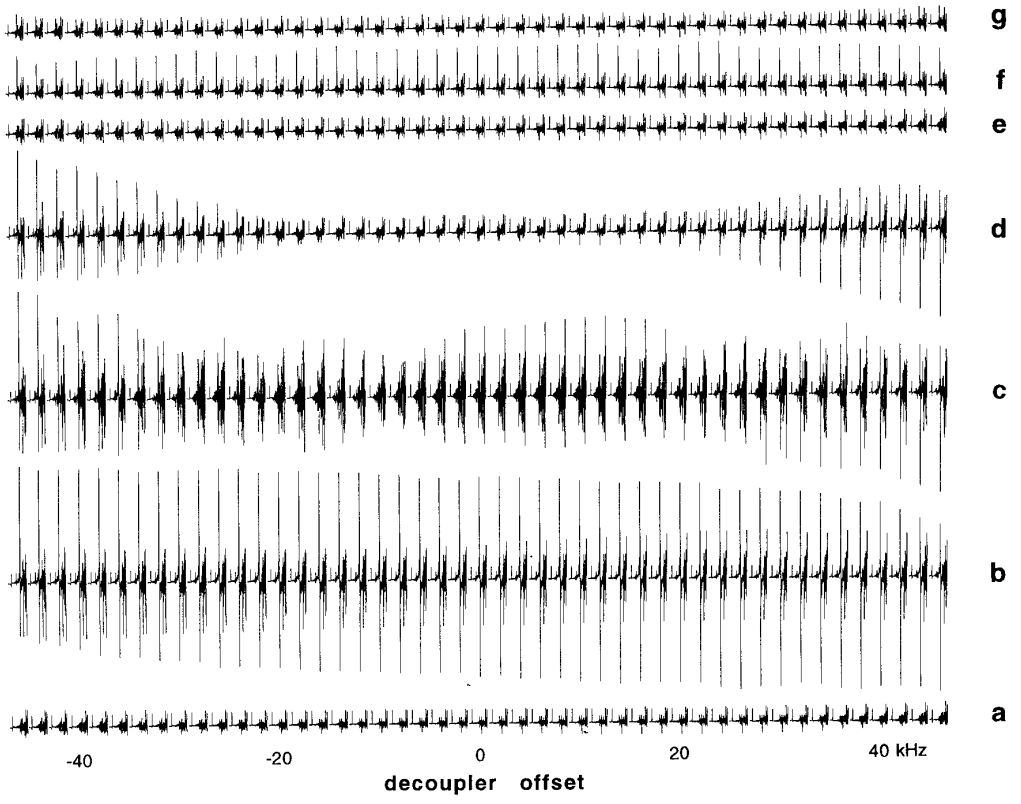

FIG. 2. Sideband levels obtained using a heteronuclear spin-echo difference pulse sequence as in Fig. 1 followed by STUD+ (*3*) decoupling (bwdth = 100 kHz, T_p = 1.0 ms, RF_{max} = 10.1 kHz) are displayed relative to the central decoupled peak in the interval 80–1170 Hz downfield from the centerband. Results at 47 different decoupler frequency offsets are shown in 2-kHz increments for each panel. (a) Ideal conditions with $\tau = 1/(2J)$, giving only in-phase S_x at the beginning of decoupling on the I spins. The effective decoupled bandwidth, where maximum sideband levels are relatively uniform and the central decoupled peak is ⩾90% of the on-resonance decoupled peak height, is >94 kHz. (b) Least ideal conditions with $\tau = 3/(4J)$, giving only antiphase S_yI_z at the beginning of I-spin decoupling for odd transients. This scenario, corresponding to real samples with a range of J couplings, produces large coherence sidebands compared to the ideal case. (c) Coherence sidebands produced by antiphase transverse coherence at the start of decoupling. As in (b) with a 90° pulse on ^{13}C (90[^{13}C], length t_{90} = 12.6 μs) to produce S_yI_y just prior to ^{13}C decoupling. This 90[I] pulse is offset with the decoupler. (d) As for (c) with a G;90[^{13}C]; $-G$ pulse train applied just prior to ^{13}C decoupling. G and $-G$ correspond to z-axis pulsed field gradients of opposite phase (length = 50 μs and amplitude = 7 G/cm). (e) As in (b) with a $90_y[^1H];G;90_{-y}[^1H]$ pulse train applied just prior to decoupling. The ^1H pulses (t_{90} = 6.3 μs) are applied on resonance. For ^1H offsets greater than ±4 kHz (the ^1H chemical shift range at 800 MHz), coherence sidebands will not be completely suppressed by this method over the large decoupled bandwidths possible using adiabatic pulses, as shown in (f). (f) As in (e) with the same high-power ^1H pulses applied 10 kHz off resonance to illustrate the performance requirements of the ^1H pulses in this method. (g) As in (b) with a $90[^{13}C];90_y[^1H];G;90_{-y}[^1H]$ pulse train just prior to ^{13}C decoupling. The 90[I] pulse is offset with the decoupler and the 90[S] pulses are applied 10 kHz off resonance. This combined method achieves complete elimination of coherence sidebands over the bandwidth necessary for a 2-GHz spectrometer, as described in the text.

configurations, but as is usual in such cases, there is an equivalent phase-cycled method. If the 90[I] pulse prior to decoupling is cycled as $90_{\pm y}$[I] for the odd transients in the spin-echo difference experiment, this generates $\pm S_yI_x$ terms in successive odd transients and achieves results that are indistinguishable from the results shown in Fig. 2d.

These two examples illustrate the effectiveness of generating opposed pairs of coherence terms which self cancel, thereby eliminating their attendant sidebands. Both methods are specific to pulse sequences which generate unwanted antiphase longitudinal coherence (S_yI_z) and are only partially successful for initial antiphase transverse coherence (S_yI_x or S_yI_y). In the G; 90[I]; $-G$ method, the I-spin magnetization, which is randomized in the transverse plane by G, is transformed to the yz plane by a 90_y[I] pulse and then the subsequent $-G$ pulse refocuses the transverse components to reform 50% of the initial I_x or I_y magnetization. On the other hand, if the antiphase I magnetization is known to be along a particular axis, and the phase of the 90[I] pulse is chosen to be orthogonal to this axis, the phase-cycled method will be effective. In some sequences the situation is simplified by preexisting phase cycling. Thus, although a non-phase-cycled HMQC sequence produces unwanted antiphase magnetization S_yI_j, where $j = x$, y, and z, the normal phase

cycling of one of the existing 90[I] pulses in the sequence eliminates any coherence sidebands from transverse magnetization, reducing the problem to one similar to the heteronuclear spin-echo sequence.

Alternatively, the S-spin components of S_yI_j coherences can be randomized by applying 90_y[S]; G; 90_{-y}[S] immediately before acquisition. In-phase S_x is preserved along the z axis, everything else is dephased by G, and then S_x is recovered by the 90_{-y}[S] pulse. This method is potentially more general, as it works on any combination of S_yI_j. As shown in Fig. 2e, coherence sidebands have been eliminated over a decoupled bandwidth of 94 kHz for I-spin decoupling. However, a high-power S pulse is necessary to achieve an increased bandwidth relative to the I-spin techniques illustrated in Fig. 2d. Although in $^{13}C^{1}H$ systems the hard 90[S] pulse only needs to excite spins over a 10 ppm ^{1}H chemical shift range compared to 200 ppm for a 90[I] pulse on ^{13}C, the I-spin methods depend on the facile conversion of I_z to transverse I_{xy} by a 90_y[I] pulse, and the increasing phase of I_{xy} with resonance offset is not important. In contrast, the S-spin technique is much more sensitive to resonance offset, as it fails when the 90_y[S] pulse significantly converts S_y to S_z.

The results in Fig. 2e were obtained with the 90[S] pulses applied on resonance. Similar results are obtained if the 90[S] pulses are shifted ± 4 kHz off resonance, which implies efficient randomization of the S spins over an offset range of 8 kHz. For S $\equiv$ ^{1}H, this is almost the maximum bandwidth required for a 1-GHz spectrometer. At larger offsets, the $1/(2T_p)$ coherence sidebands exceed the maximum normal sidebands, as shown in Fig. 2f for 90[S] pulses 10 kHz off resonance.

To eliminate coherence sidebands over a greater decoupled bandwidth, the I- and S-spin methods may be combined as 90_y[I]; 90_y[S]; G; 90_{-y}[S]. For antiphase S_yI_z or S_yI_y, the sidebands are decreased by the randomization of both I and S magnetization, and the two resulting reduction factors are multiplied together. This is illustrated in Fig. 2g for the same S-spin offset (10 kHz) shown in Fig. 2f, where the 90[S] bandwidth for ideal transformation of S spins was insufficient to eliminate coherence sidebands. The resulting sideband levels in Fig. 2g are indistinguishable from levels in Fig. 2a with no coherence sidebands. Thus, the complete elimination of coherence sidebands over resonance offsets greater than ± 47 kHz for I spins, with S spins offset 10 kHz, implies that the combined method achieves the necessary transformations of S(^{1}H) and I(^{13}C) spins over ± 10 and ± 50 kHz, respectively, sufficient for a 2-GHz spectrometer.

Coherence sidebands in adiabatic decoupling result from the presence of S_yI_j ($j = x, y, z$) terms at the start of signal acquisition. We have provided three simple methods which eliminate these sidebands in a single transient using pulsed field gradients, over bandwidths of up to 100 kHz. These techniques are based on generating $\pm S_yI_j$ pairs which cancel prior to decoupling. In addition to these methods, high-power adiabatic pulses can be successfully employed as the first elements of a decoupling scheme to randomize the undesired coherence terms across the sample using the residual inhomogeneity of the RF probe. Alternatively, such an additional broadband adiabatic inversion pulse can be used on alternate transients to invert S_yI_j. We also note that the requirements for the suppression of coherence sidebands which arise from adiabatic decoupling will differ between pulse sequences. Indeed, multiple-dimensional NMR sequences which employ sensitivity enhancement rely on the detection of both S_x and S_y magnetization, so S-spin suppression methods would be inappropriate in these cases. Detailed analyses of these and related topics will be presented in a subsequent treatment.

ACKNOWLEDGMENTS

We thank the reviewers for calling our attention to the work cited in Refs. (*2, 6*).

REFERENCES

1. T. E. Skinner and M. R. Bendall, *J. Magn. Reson. A* **123,** 111 (1996).
2. A. Bax, G. M. Clore, P. C. Driscoll, A. M. Gronenborn, M. Ikura, and L. E. Kay, *J. Magn. Reson.* **87,** 620 (1990).
3. T. E. Skinner and M. R. Bendall, *J. Magn. Reson.* **124,** 474 (1997).
4. E. Kupce, R. Freeman, G. Wider, and K. Wuthrich, *J. Magn. Reson. A* **122,** 81 (1996).
5. D. T. Pegg, M. R. Bendall, and D. M. Doddrell, *J. Magn. Reson.* **49,** 32 (1982).
6. M. H. Levitt, G. Bodenhausen, and R. R. Ernst, *J. Magn. Reson.* **53,** 443 (1983).
7. M. R. Bendall, D. T. Pegg, D. M. Doddrell, and J. Field, *J. Am. Chem. Soc.* **103,** 934 (1981).
8. J. S. Waugh, *J. Magn. Reson.* **50,** 30 (1982).